FlashCam: A high-performance camera for IACTs

Clara Escañuela Nieves[1,*], *Miquel* Barcelo[1], *Christian* Bauer[1], *Baiyang* Bi[2], *Sebastian* Diebold[2], *Christian* Föhr[1], *Stefan* Funk[3], *Fabian* Haist[1], *German* Hermann[1], *Bastian* Heß[2], *Jim* Hinton[1], *Ira* Jung-Richardt[3], *Oleg* Kalekin[3], *Thomas* Kihm[1], *Gerd* Pühlhofer[2], *Olaf* Reimer[4], *Simon* Sailer[1], *Andrea* Santangelo[2], *Thomas* Schanz[2], *Pedro* Silva Batista[3], *Simon* Steinmassl[1], *Christoph* Tenzer[2], and *Felix* Werner[1]

[1]Max-Planck-Institut für Kernphysik, Saupfercheckweg 1, 69117 Heidelberg, Deutschland
[2]Eberhard Karls Universität Tübingen, Geschwister-Scholl-Platz, 72074 Tübingen, Deutschland
[3]Erlangen Centre for Astroparticle Physics, FAU Erlangen-Nürnberg, Nikolaus-Fiebiger-Straße 2, 91058 Erlangen, Deutschland
[4]Universität Innsbruck, Innrain 52, 6020 Innsbruck, Österreich

Abstract. FlashCam is an advanced camera developed for Imaging Atmospheric Cherenkov Telescopes (IACTs), aiming to significantly enhance ground-based astronomical observations. FlashCam has delivered exceptional performance within the High Energy Stereoscopic System (H.E.S.S.) for over 5 years. Its design has been thoroughly studied using laboratory data as well as accurate simulations, all of which show good agreement between simulated and observed results. Minor adjustments are being made to the camera design in preparation for its integration with the Cherenkov Telescope Array Observatory (CTAO).
Calibration is a critical aspect of any detector, and muons provide an effective means to calibrate the telescope's full optical throughput. For FlashCam, a specialized muon detection method achieves over 95% efficiency in identifying muons, with a low background acceptance.

1 Introduction

FlashCam is a high-speed, photomultiplier (PMT)-based camera optimized for nanosecond-resolution imaging, designed for IACTs [1]. FlashCam design and performance has been fully tested and verified with extensive laboratory testing. These tests have confirmed a strong agreement between laboratory data and simulation models. Following its installation on the large (mirror area 600 m^2) central telescope of the H.E.S.S. array [2], FlashCam has gained field experience over the last 5 years leading to significant scientific insights.

FlashCam is a candidate for the Medium-Sized Telescopes (MSTs) within the Southern array of the CTAO [3]. In preparation for a pathfinder, minor design modifications have been made to enhance both reproducibility and monitoring capabilities. Additionally, data analysis techniques are being adapted to support upcoming observations, alongside the development of essential methods for data calibration, scientific analysis, and data handling.

Muons are a crucial tool for the calibration of the optical efficiency of the complete telescope, including the camera. This calibration is performed only with fully-contained ring-shaped muon images. To ensure effective calibration, muon ring detection must occur online, as events that uniquely trigger on one telescope are stored only when tagged as muon rings. In this contribution we present a simple muon tagging method for FlashCam based on the trigger system.

*e-mail: clara.escanuela@mpi-hd.mpg.de

2 FlashCam

FlashCam has a fully-digital readout and trigger system and a walk-in mechanics. Its horizontal architecture is divided in three sections: the photon-detector plane (PDP), readout electronics, and data acquisition system (DAQ). FlashCam consists on 1764 pixels, of which 1761 are equipped with PMTs, that are arranged in groups of 12 which lead to a total of 147 PDP modules. A transparent window and shutter shield the PDP. In front of the PMTs, Winston cones enhance light collection and reduce the dead space between pixels.

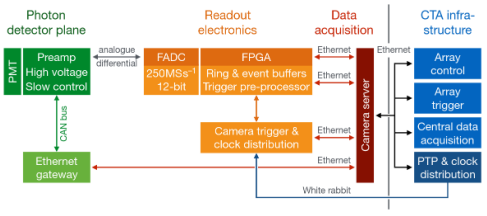

Figure 1: Schematic of the functioning of FlashCam [1].

Each PDP module contains a DC-DC converter that provides high-voltage to each PMT. Additionally, every PDP module is equipped with pre-amplifiers and a CAN bus interface, enabling slow control, monitoring, and safety functions, as shown in Fig. 1. Photons hitting the photocathode of a PMT get converted with a certain quan-

tum efficiency into photoelectrons (PEs) resulting in an electric pulse on the analogue signal output. The method of signal amplification varies based on the intensity of the signal. Above 250 PEs, signals saturate in a controlled way to reach a dynamic range of up to 3000 PEs.

Analogue signals are transmitted towards the readout system and are continuously digitised at a rate of 250 MSamples/sec via 12-bit Flash ADCs (FADCs). Samples are buffered in FPGAs until the trigger decision is achieved. The front-end electronics consist of motherboards that include 84 FADC modules, 12 trigger cards, and a master distribution board responsible for distributing a common clock and trigger signals.

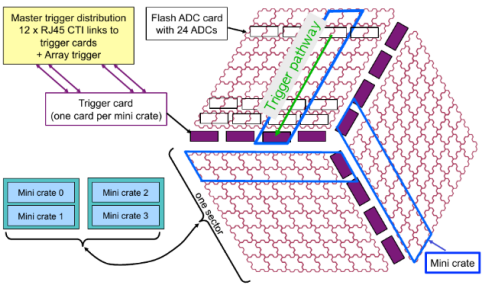

Figure 2: FlashCam signal chain [4] which shows the configuration of FADC cards, 12 trigger cards, and PDPs. The trigger decision is transmitted to the trigger card through the mini crate and sent to the master trigger distribution.

The trigger system [4] is designed to reliably detect small images consisting of only a few pixels, maintaining a stable false positive rate even under high Night Sky Background (NSB) conditions. Fig. 2 shows the trigger pathway of the camera. The camera is composed of three sectors, each made of 4 mini-crates and 4 trigger cards. On the FADC level, an integer differentiation filter is applied to the electric pulses to enhance the rising edge. The pulses are also clipped to reduce the dynamic range. Moreover, three channels are summed up to form three-pixel sums and then divided by 2 to limit again the number of bits to transfer to the associated trigger card. Each 3-pixel sum is summed up again to lead to 9-pixel patches. Patches overlap with each other leading to a maximum of 588 patches. The patch sum triggers if it exceeds a threshold. The outcome of this check is encoded into a 1-bit signal, which is transmitted from the trigger cards to the master distribution board.

2.1 FlashCam in H.E.S.S.

FlashCam was installed in the large central telescope in H.E.S.S. in the fall of 2019 and has been in continuous operation since then, with an uptime of approximately 98%. After a period of verification measurements including studies on Monte Carlo and data consistency, camera stability, and the observation of scientific verification targets, routine science operation started already 1 month after installation [5].

The consistency of Monte Carlo simulations and data was validated in the laboratory prior to 2019 [4] and subsequently verified with real data. The trigger rate, both in simulations and in real data from the telescope, has been shown to be consistent after making a few minor adjustments [6]. The stability of the camera response over the years is further highlighted by the stable behaviour of the camera monoscopic trigger rate (Fig. 3).

Following the initial 15 sigma detection of the Crab Nebula already 3 days after installation, a scientific verification program was conducted, which included additional observations of science targets to validate the performance [7]. As presented in detail in [8], the Crab Nebula spectrum derived with a monoscopic analysis based on FlashCam data is consistent with the spectrum derived with a stereoscopic reconstruction method using the other H.E.S.S. telescopes, as well as consistent with the spectrum derived with other instruments. The FlashCam data allows an extension of the detected H.E.S.S. spectrum to lower energies, which was also utilized in other works such as the detection of the recurrent Nova RS Ophiuchi [9].

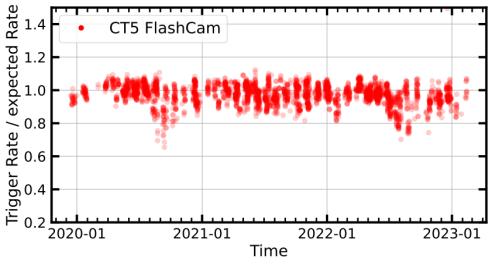

Figure 3: Stability of the trigger rate with respect to time from January 2020 to 2023.

3 Muon tagging

3.1 Muon calibration

The CTAO aims to detect very-high-energy gamma rays with unprecedented sensitivity and resolution, significantly increasing observational coverage across the energy range. To meet stringent energy reconstruction accuracy requirements, precise calibration is essential. This includes achieving a good understanding of photon transmission through the detector and their conversion to photoelectrons.

Atmospheric muons are mostly produced by hadronic interactions and are characterized by their high penetration depth and nearly straight-line trajectory. In air, muons undergo little scattering and the refractive index is almost constant at heights below 1.5 km above ground [10]; consequently, muons emit Cherenkov light at an almost constant angle as they pass through the medium. When a muon traverses a mirror dish [11], Cherenkov light is collected by the camera, resulting in the formation of a dis-

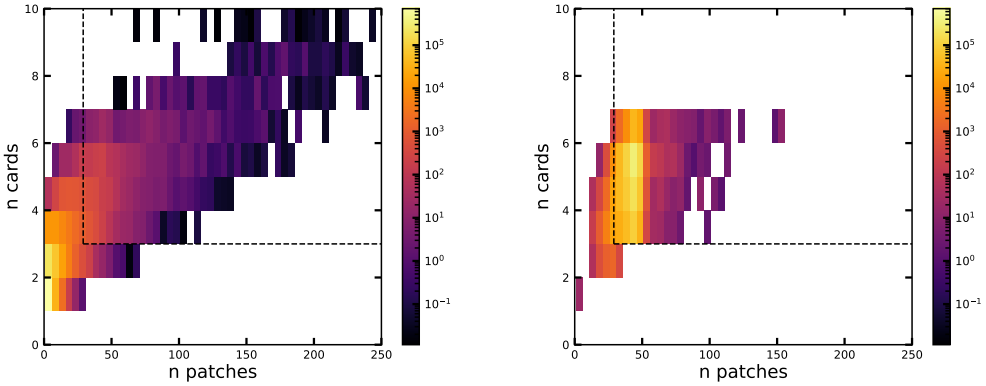

(a) All particles.

(b) Muon rings at energies ≥ 20 GeV.

Figure 4: Number of triggered patches and cards using simulations.

tinctive ring-shaped image. As the offset of the muon trajectory with respect to the optical axis of the telescope increases, the centre of the muon ring shifts away from the centre of the telescope mirror.

The reconstruction of the muon ring radius gives an estimation of the yield of emitted photons which allows the prediction of the number of photoelectrons each PMT expects. By comparing the expected and observed photoelectron counts per PMT, one can calibrate the entire optical throughput. Muon calibration can be conducted continuously and during observations.

3.2 Muon identification

The CTAO will store an event only if there are simultaneous triggers from more than two telescopes. Therefore, muons that only trigger one telescope would be lost. However, due to the critical role of muons in IACTs, the CTAO requirements allow each telescope to transmit up to 1400 Hz of monoscopic events. This rate includes not only potential muon events but also other essential calibration data, such as flat-fielding information. Muon tagging algorithms must process each event to detect observable muon rings. Given the high event rate, a rapid and efficient method is essential for promptly verifying the presence of muon rings within the data stream.

Muon ring-shaped images trigger on larger areas of the camera compared to typical low-energy showers. At least $2\pi\frac{\theta_c}{\omega} \approx 50$ pixels are triggered assuming only one row of pixels is illuminated, a Cherenkov angle of $\theta_c = 1.23°$ and a pixel field of view of $\omega = 0.18°$. Each muon event generates a signal that is fully contained within a single time sample (of 4 ns for FlashCam) after the first pixel triggers. In contrast, signals from shower-induced events typically exhibit a longer time spread, often spanning more than two samples. The number of triggered patches and cards within one or two time samples is a distinct signature to distinguish muons from background signals. Background sources include cosmic rays, gamma rays, and non-ring-producing muons. Fully-contained muon rings are produced when the impact distance, the distance from centre of muon ring to the centre of the dish is ≤ 4 m and the offset (v), angle from the direction of telescope is $\leq 2.6°$ according to $v + \theta_c \leq \frac{\text{fov}}{2}$ [10]. fov is the field of view of the camera, between 7° and 7.7°.

A fast method of muon detection relies on the trigger system [12] with only two variables used: number of triggered 9-sum patches and cards, as explained at the end of Section 2. The number of patches that exceed a constant trigger threshold can be counted together with the number of cards that register at least one triggered patch. There are a total of 588 patches and 12 trigger cards.

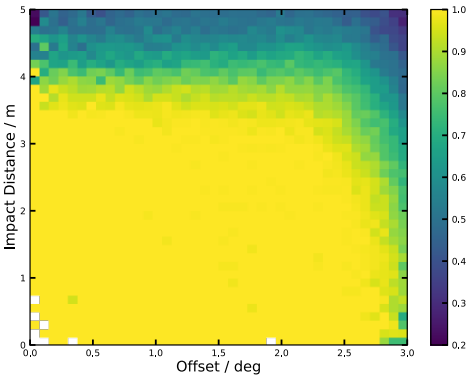

Figure 5: Muon detection efficiency with impact distance and angle offset for muons with energy ≥ 20 GeV.

The timing of the trigger for each patch can enhance our ability to distinguish between signal and background. We count the number of patches that trigger within a certain number of samples (sufficient to capture all triggered

patches for muons) after the first triggered patch. The time difference between the first and last triggered patch for a muon generally falls within a single sample of the readout. However, if the first trigger occurs just before a sample ends, the next pixel trigger can happen in the next sample so that the muon triggers two samples. Therefore, patches are counted within the first two samples after the trigger.

Muon and shower images are generated from simulations with sim_telarray [13] and CORSIKA [14]. Fig. 4 shows a 2D histogram of events binned by the number of triggered cards and patches. The dashed lines show the cuts in patches and cards made to achieve good signal efficiency and low false positive rate. Fig. 4a shows the distribution of all events using proton simulations and Fig. 4b shows muons after cuts on impact distance and offset to ensure fully-contained rings. Fig. 5 shows the efficiency of detecting ≥ 20 GeV muons with respect to impact distance and offset that trigger on at least 30 patches and 3 cards. The efficiency clearly degrades with impact distance.

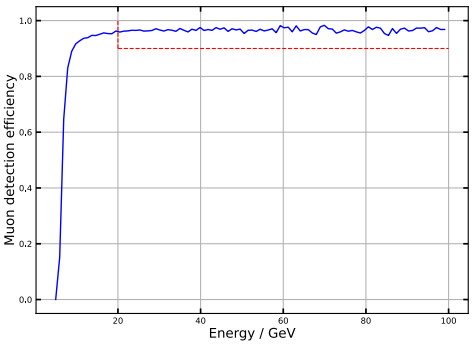

Figure 6: Muon detection efficiency as a function of the particle energy. Red dashed line: CTAO requirements.

The CTAO requirements indicate that muon efficiency must be higher than 90% for ≥ 20 GeV as shown by the red dashed lines of Fig. 6. The detection efficiency of muon rings is higher than 95% from an energy of 10 GeV. Additionally, after applying trigger cuts, we end up with less than 2% of background events. The total rate of monoscopic events that pass muon tagging is at most a few hundred events per second, well below the maximum of 1400 Hz. For this study, the maximum impact distance of muons has been set to 4 m. However, reducing the cut in the number of patches to 25 reaches a muon detection efficiency ≥ 90% for muon rings with an impact distance cut extended to 5 m while still keeping low background acceptance.

4 Conclusion

The advanced FlashCam prototype operated within H.E.S.S. has shown great reliability with an uptime of 98% over 5 years of operation, significantly improving the availability of 5-telescope data probing the full very-high-energy gamma-ray regime. A good understanding of the camera response with regards to both, data as well as simulations, is proved. FlashCam performance is shown to be well understood and suited for the MST telescopes of CTAO-South. A simple trigger-based muon tagging algorithm has been developed and identifies over 90% of muon rings and low background rate.

References

[1] F. Werner et al., Performance verification of the FlashCam prototype camera for the Cherenkov Telescope Array, Nuclear Instruments and Methods in Physics Research Section A: Accelerators, Spectrometers, Detectors and Associated Equipment **876**, 31 (2017).

[2] B. Bi et al., Performance of the New FlashCam-based Camera in the 28\, m Telescope of HESS, arXiv preprint arXiv:2108.03046 (2021).

[3] S. Vercellone, C. Consortium, The next generation Cherenkov Telescope Array observatory: CTA, Nuclear Instruments and Methods in Physics Research Section A: Accelerators, Spectrometers, Detectors and Associated Equipment **766**, 73 (2014).

[4] S. Sailer, Ph.D. thesis (2020)

[5] S. Steinmaßl, Ph.D. thesis, Ruprecht-Karls-Universität Heidelberg (2023)

[6] F. Leuschner et al., Validating Monte Carlo simulations for an analysis chain in HESS, arXiv preprint arXiv:2303.00412 (2023).

[7] G. Pühlhofer et al., Science verification of the new FlashCam-based camera in the 28m telescope of HESS, arXiv preprint arXiv:2108.02596 (2021).

[8] F. Aharonian et al., Spectrum and extension of the inverse-Compton emission of the Crab Nebula from a combined Fermi-LAT and H.E.S.S. analysis, AA **686**, A308 (2024). 10.1051/0004-6361/202348651

[9] HESS Collaboration, Time-resolved hadronic particle acceleration in the recurrent nova RS Ophiuchi, Science **376**, 77 (2022).

[10] M. Gaug et al., Using muon rings for the calibration of the Cherenkov telescope array: a systematic review of the method and its potential accuracy, The Astrophysical Journal Supplement Series **243**, 11 (2019).

[11] G. Vacanti et al., Muon ring images with an atmospheric Čerenkov telescope, Astroparticle Physics **2**, 1 (1994).

[12] F. Werner, Fast, software-based muon tagging with FlashCam, https://www.mpi-hd.mpg.de/personalhomes/fwerner/research/2021/08/fast-muon-tagging-flashcam/

[13] K. Bernlöhr, Simulation of imaging atmospheric Cherenkov telescopes with CORSIKA and sim_telarray, Astroparticle Physics **30**, 149 (2008).

[14] D. Heck et al., CORSIKA: A Monte Carlo code to simulate extensive air showers (1998).